

# *Evidence of Shelfal Hyperpycnal Deposition of Pliocene Sandstones in the Oilbird Field, Southeast Coast, Trinidad: Impact on Reservoir Distribution*

**Helena Gamero Diaz and Carmen Contreras**

*Schlumberger Technology Corp., Addison, Texas, U.S.A.*

**Neil Lewis and Robert Welsh**

*EOG Resources Trinidad Limited, Port of Spain, Trinidad and Tobago*

**Carlos Zavala**

*GCS Argentina, Universidad Nacional del Sur, Bahía Blanca, Argentina*

## **ABSTRACT**

**T**he Pliocene B4 sandstone is an important gas-bearing reservoir in the Oilbird field, Columbus Basin, southeast Trinidad. The B4 sandstone is dominated by fine-grained, massive, and parallel-laminated sandstones interbedded with thinly laminated siltstone and very fine-grained sandstones deposited in a shelfal setting. A detailed sedimentologic study of the B4 reservoir was performed by integrating 60 ft (18.3 m) of core, 3770 ft (1149 m) of borehole image data, open-hole logs, mud logs, and biostratigraphic data. A total of 12 sedimentary facies were described and interpreted on the basis of sedimentation processes using a genetically oriented facies analysis approach. Six facies associations were identified based on the gamma ray (GR) pattern and the vertical facies association. Core data show mostly massive sandstones with very little to no bioturbation. These massive sandstones commonly alternate with intervals having diffuse lamination, which appear as a recurrent feature within the massive bodies. The transitional recurrence of massive and parallel-laminated sandstones indicates velocity fluctuating and sustained turbulent flows. Sedimentologic evidences suggest that the origin of the B4 sandstone could be related to the paleo-Orinoco River-related

product of turbidity (hyperpycnal) outflows that extended into the Columbus Basin. The associated occurrence of plant debris favors the interpretation of a direct fluvial supply by rivers in flood stage (hyperpycnal systems).

The lateral correlation of facies associations throughout seven wells allowed the identification of six depositional units, named from base to top, A, B, C, D, E, and F. Facies maps for the B4 reservoir have been developed and were constrained by paleocurrent data extracted from image data. The B4 reservoir sand shows a progradational pattern reflecting the infill of a fault-controlled depocenter. Paleoflow data indicate axial transport roughly parallel to the main fault system, indicating that faults were active and controlled the accommodation space. The proposed hyperpycnal depositional model will introduce substantial changes for the prediction of the geometry and position of sandstone accumulations. The hyperpycnal model predicts the occurrence of sand accumulations in the lower parts of the paleolandscape, whereas the higher parts of the basin (margins) are characterized by fine-grained sediments. Thus, this new depositional model could represent a drastic shift in the prospectivity guide for new exploration plays.

## INTRODUCTION

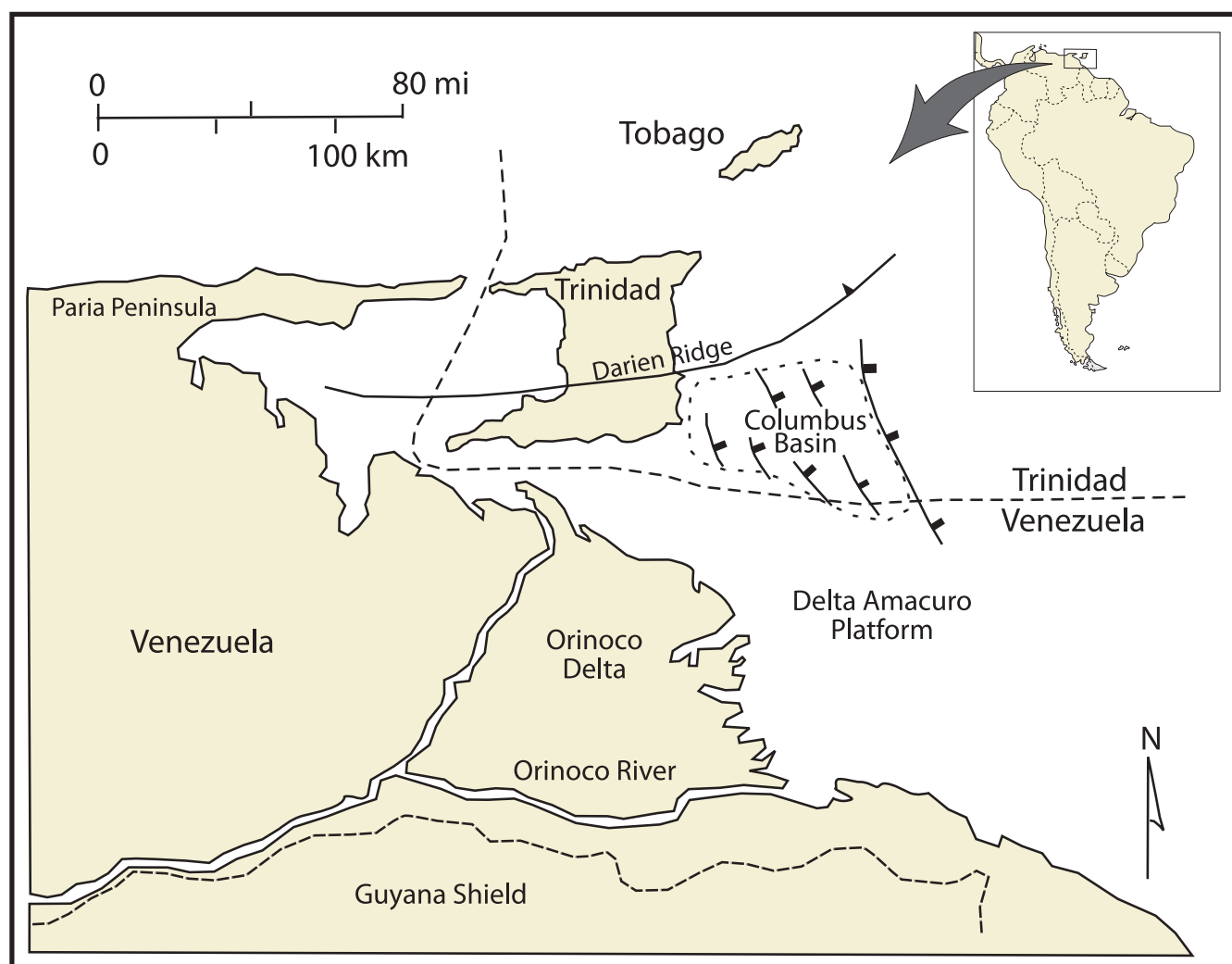
Located southeast of Trinidad, the Columbus Basin is one of the most prolific petroleum basins of the Caribbean region. Main hydrocarbon reservoirs are highly porous and very thick fine-grained sandstones that accumulated during the Late Miocene and Pliocene. These deposits have been related to wave-dominated littoral deltas associated with an ancient big river located to the west, known as the paleo-Orinoco. The interpretation of sandstone deposits as wave-dominated delta-front accumulations led to several problems in explaining the occurrence of these sandstones:

- 1) If these sandstones belong to littoral deltas, relative sea level changes should be an important factor allowing the high-frequency progradation-retrogradation of delta-front and associated delta-plain deposits for more than 200 km (656,167 ft). However, delta-plain facies have never been recognized in cores nor in outcrops.
- 2) Although wave-dominated deltas are characterized by shoreface deposits with abundant wave ripples, these sandstones commonly lack any evidence of wave-reworking processes.
- 3) Facies analysis of core and borehole image data from Pliocene deposits of the Oilbird field allowed revision of the origin and significance of sandstone reservoirs. Main sandstone facies show depositional features that suggest an accumulation from long-lived sediment gravity flows. In this chapter, an alternative interpretation for the origin of sandstone deposits is proposed, related to

an accumulation by hyperpycnal flow deposits in a marine shelfal setting.

## GEOLOGIC FRAMEWORK

The Columbus Basin is located offshore southeast Trinidad in a zone of intense strike-slip deformation as a result of the oblique collision between the Caribbean and South American plates (Leonard, 1983; Robertson and Burke, 1989; Babb and Mann, 1999; Wood, 2000; Gibson et al., in press). This basin has an overall triangular shape and is limited by the Darien Ridge to the north, the Atlantic continental shelf to the east, the onshore southern Trinidad to the west, and the Amacuro shelf of Venezuela to the south (Figure 1). From a regional scale, the Columbus Basin is situated on the South American plate just south of its boundary with the Caribbean plate (Gibson et al., in press), which is moving eastward relative to South America and the Atlantic basin. The east-west-trending Caribbean-South American margin is characterized by a late Oligocene to middle Miocene transpressional thrust belt (Serranía del Interior Oriental of Venezuela and Central and Northern Ranges of Trinidad). This thrust belt continues offshore into the eastern shelf of Trinidad north of Point Radix into Darien Ridge and joining the Barbados accretionary prism beyond the modern shelf edge. The Miocene thrust front effectively defines the northern boundary of the Columbus Basin. The foreland basin associated with this deformed belt consists of the Eastern Venezuela Basin, which evolves eastward into the Columbus Basin. Foreland basin subsidence in eastern Venezuela



**FIGURE 1.** Location map of the Columbus Basin (modified after Wood, 2000).

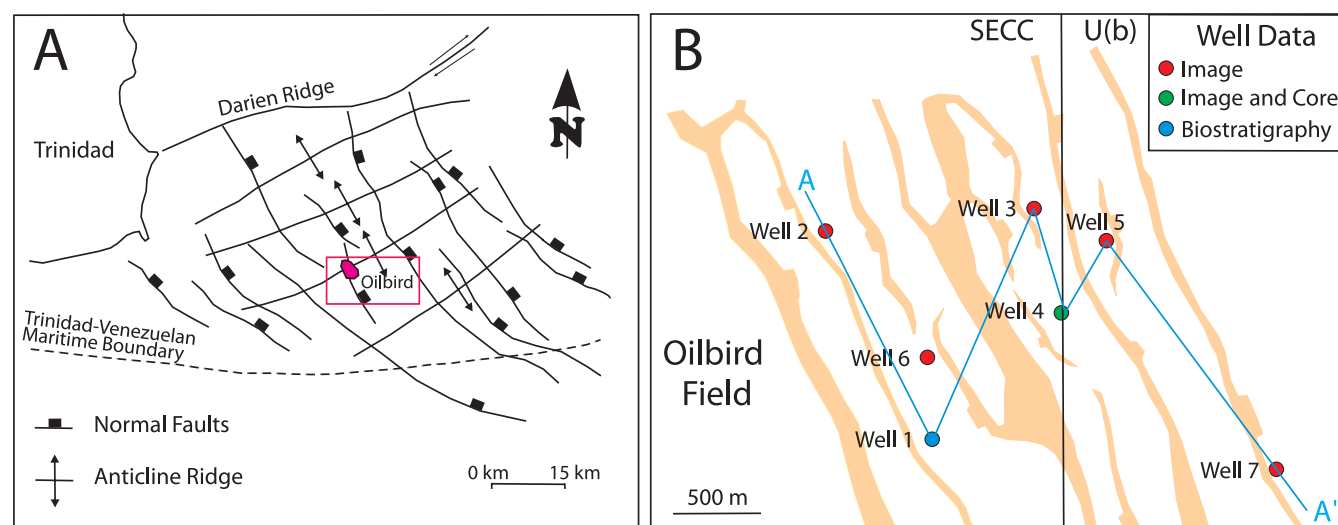
and Trinidad began in the late Oligocene to early Miocene (Pindell et al., 1998), culminating with the emplacement of the Serrania del Interior Oriental–Central Range thrust belt in early Miocene. This thrusting came to an end by the late middle Miocene when the Caribbean–South American relative plate motion changed from transpression to transtension. Throughout the Late Cretaceous, widespread deposition of the petroleum-rich source rock occurred, and it is this source rock that is responsible for the generation of almost all the petroleum in Venezuela and Trinidad.

During the Pliocene–Pleistocene, the basin evolved into a thin-skinned, pull-apart basin that captured shallow-water sedimentary deposits of the prograding paleo-Orinoco River delta (Gibson et al., in press). Pliocene–Pleistocene structures within the basin include large-magnitude northwest–southeast-oriented down-to-the-northeast extensional faults, northeast–

southwest-trending contractional folds, and strike-slip fault systems, all of which are regionally detached near the top of the underlying north-dipping passive margin succession. At the end of the middle Miocene, the north-draining paleo-Orinoco River was diverted eastward along the axis of the foreland basin by the growing Serrania–Central Range thrust belt (Diaz de Gamero, 1996). Since the late Miocene, the Columbus Basin area has been the depocenter for Orinoco-derived sediments exceeding 9150 m (30,000 ft) in thickness (reported sedimentation rates are between 5 and 10 m [16 and 33 ft]/1000 yr).

### *The Oilbird Field*

The Oilbird field is located within the South East Coast Consortium Block some 40 km (25 mi) southeast of Trinidad's mainland (Figure 2). It sits within the Columbus Basin, which has produced significant



**FIGURE 2.** (A) Main structural elements of the Columbus Basin (modified after Wood, 2000). The Columbus Basin is characterized by two sets of structural elements: (1) northwest–southeast-oriented down-to-the-northeast extensional faults and (2) northeast–southwest-trending contractional folds (Leonard 1983; Wood, 2000). (B) Map of the Oilbird field showing the location of the wells used in this study, and regional cross section AA', shown in Figure 11. SECC = South East Coast Consortium; U(b) = concession block held and operated by EOG Resources Trinidad Limited.

quantities of oil and gas since the first offshore oil discoveries during the early 1970s. The Columbus Basin is characterized by a prolific Cretaceous source rock with main associated reservoirs located in the Tertiary sand-rich shelfal stratigraphic section. The structural evolution of the basin has created abundant hydrocarbon traps, along with an efficient petroleum migration system. Proven and probable gas reserves at the end of 2008 stood at approximately 23.8 tcf.

The Oilbird field was discovered in 1977 by Texaco with the drilling of the Oilbird-1 well (well 1, Figure 2B). At that time, natural gas had no economic value, so appraisal drilling only occurred in 2001–2002. Platform installation occurred in late 2006, followed by the drilling of five additional development wells.

The B4 Pliocene sandstone is an important gas-condensate-bearing reservoir in the Oilbird field (Figure 3). Figure 3 shows the main reservoir sandstones in the Oilbird field. The B4 sandstone is dominated by fine-grained, massive, and parallel-laminated sandstones interbedded with thinly laminated siltstone and very fine-grained sandstones, which have been interpreted as deposited by a shelf-edge delta system (Bowman, 2003; Bowman and Johnson, 2006).

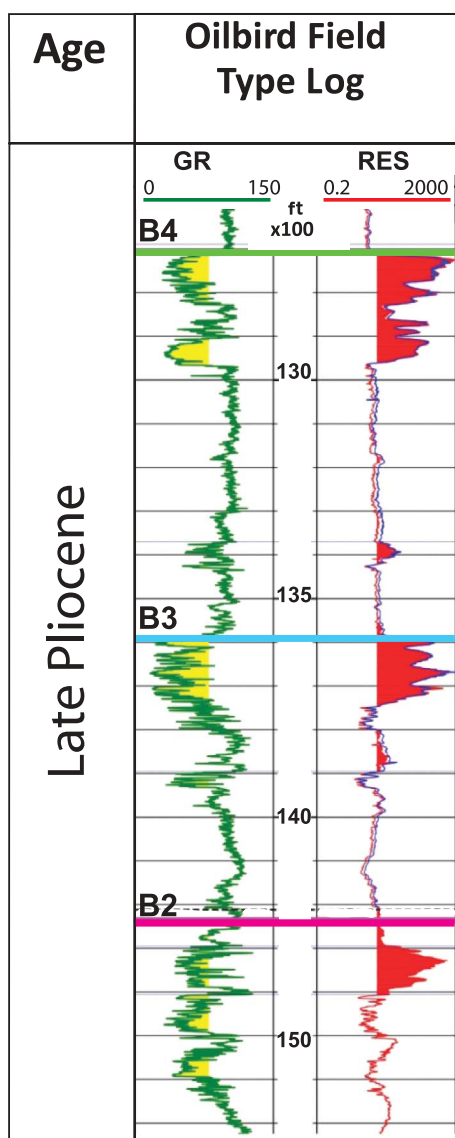
The analysis of core data shows a dominance of very well-sorted fine-grained sandstones, which are massive or show planar lamination with abundant plant debris. These sandstones are composed of very thick packages internally showing gradual recurrences of facies, thus indicating an origin related to sus-

tained, long-lived, and fluctuating turbulent flows (Zavala et al., 2006c; Lamb et al., 2008; Jackson et al., 2009; Lamb and Mohrig, 2009). The association of massive and laminated sandstones is now considered diagnostic features originated by the collapse of sand-rich turbulent suspensions under different rates of sediment fallout (Arnott and Hand, 1989; Kneller and Branney, 1995; Sumner et al., 2008).

In this chapter, we propose an alternative interpretation for the origin of B4 sandstone deposits as related to an accumulation by hyperpycnal flows in marine shelfal areas. This interpretation is based on the analysis of facies and sedimentary features in the B4 Oilbird sandstones supported by core, log, and borehole electrical image data. High-resolution borehole images provide paleocurrent orientations that complemented the depositional model built from the facies analysis of cores.

### Previous Work

Pliocene–Pleistocene sandstones of the Columbus Basin have been previously interpreted as accumulated by wave-dominated littoral deltas, characterized by extensive prograding shoreface/shelfal deposits (Wood, 2000; Wood and Roberts, 2001) and by shelf-edge deltas (Bowman, 2003; Bowman and Johnson, 2006). Wood (2000) established that the Columbus Basin was filled throughout the Pliocene and Pleistocene by more than 12 km (7.4 mi) of clastic sediments supplied by the paleo-Orinoco delta system.



**FIGURE 3.** Type log of the Late Pliocene Oilbird sandstone reservoirs. The B4 sandstone is a gas-condensate reservoir. GR = gamma ray in API units; RES = resistivity in ohm m units.

The model proposed by Wood (2000) shows fluvial-dominated deltas feeding, wave-dominated strand-plain shoreline systems. Ultimately, strand-plain/shoreface deposits form elongated sand bodies oriented parallel to the coastline.

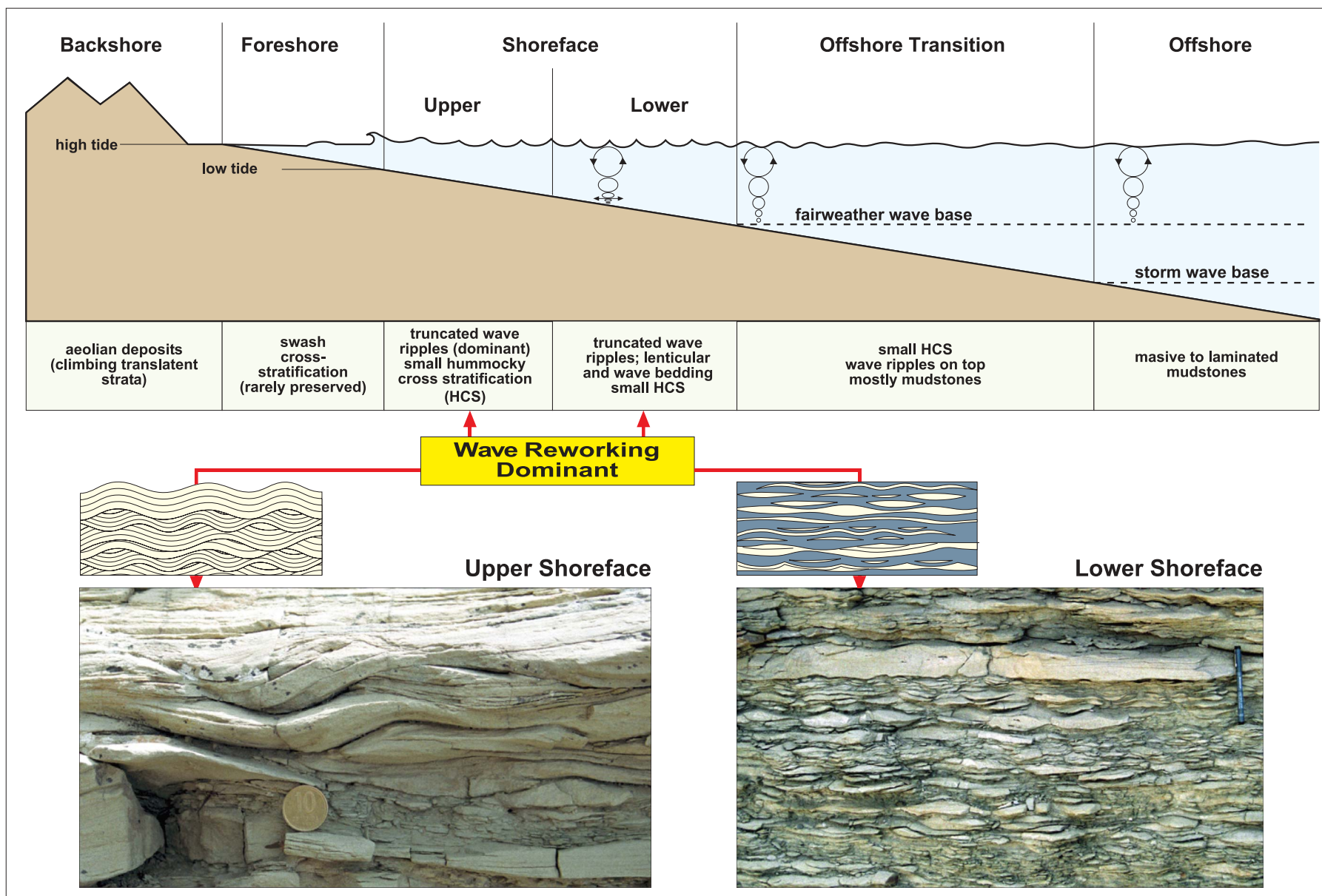
From a sedimentologic standpoint, the shoreface is a nearshore area located between the lowest tide and the wave base. Typical shoreface deposits are characterized by sandstone and mudstone layers composed of rhythmic heterolithic successions showing abundant wave-related sedimentary structures. The sand/shale ratio allowed the distinction of upper, middle, and lower shoreface deposits. The passage be-

tween the lower shoreface and the offshore transition is marked by the fair-weather wave base, which separates the high-energy coastal zone from the more internal areas characterized by mudstone accumulations commonly punctuated by storm deposits. Consequently, classic shoreface deposits are composed of sandy layers with flaser and truncated wave ripples reflecting wave action, a dominant process in a shoreface (Figure 4). Sedimentary structures, such as microhummocky cross-stratification, are also common and are considered diagnostic features of storm deposition in the shoreface (Walker, 1996).

The interpretation of a storm- or wave-dominated shoreface environment in the Columbus Basin was supported by faunal assemblages that reflect shallowing-upward conditions, as well as the existence of clean, massive, and parallel-laminated sandstones interbedded with levels showing hummocky cross-stratification and *Ophiomorpha* burrows. Nevertheless, no diagnostic structures of wave activity as wave-truncated ripples were described.

Bowman and Johnson (2006) proposed that the Pliocene-Pleistocene sandstones in the Columbus Basin were deposited by shelf-edge delta systems. They concluded that under conditions of high sediment supply and accommodation space, deltas in the shelf edge may generate thick delta slope and delta-front successions, more than 340 m (1115 ft) thick. The shelf-edge deltas were deposited within the structurally generated accommodation space between syndepositional northeast- and southwest-dipping normal faults (Gibson et al., in press). Wood (2000) and Bowman and Johnson (2006) established the Sao Francisco delta, offshore Brazil, and the Orinoco delta, Venezuela, respectively, as modern analogs for the Pliocene-Pleistocene deposits in the Columbus Basin. Although littoral delta systems are commonly preserved in the geologic record, the associated sandstone deposits in the delta front are commonly relatively thin (<5 m [16 ft]) because of the strong energetic control and the limited available accommodation space in coastal areas. Nevertheless, recent studies support the common occurrence of very thick clastic successions associated with submarine deltas (in the sense of Bates, 1953). These submarine deltas compose a new type and poorly known fluvial-related depositional system termed hyperpycnal systems (Zavala et al., 2006c; Zavala et al., 2011) capable of transporting huge volumes of sediment into the basin and accumulating very thick deposits having diagnostic structures commonly confused with shoreface deposits.





**FIGURE 4.** Depositional characteristics of shoreface deposits (C. Zavala, 2007, personal communication). Main sedimentary structures diagnostic of lower-to-upper shoreface environments. The dominant process in the shoreface is wave action, with truncated wave ripples being the most characteristic sedimentary structure in this environment.

### ***Hyperpycnal Systems: New Depositional Models***

A hyperpycnal system is the subaqueous extension of the fluvial system (Zavala et al., 2006c). It originates when excess in density causes a sediment-laden fluvial discharge to plunge below the receiving water body (Bates, 1953; Mulder and Alexander, 2001), mainly during flood conditions. During these periods, huge volumes of clastics are commonly transferred into the basin by a subaqueous extension of the fluvial system (in the sense of Schumm, 1981). The resulting deposits are termed “hyperpycnites” (Mulder et al., 2003) and constitute a land-generated turbulent flow deposit commonly associated with long-lived and quasi-steady flow discharges. These deposits have poorly known facies and facies associations. Although ancient hyperpycnal deposits are poorly documented in the literature, some advances have appeared in recent publications, referring to both ancient and modern successions (Mulder and Alexander, 2001; Mulder et al., 2003; Nakajima, 2006; Zavala et al., 2006c; Zavala et al., 2011). Recently, hyperpycnal flows are receiving more attention as efficient mechanisms for transporting enormous quantities of sands into a basin (Mutti et al., 1996; Mulder and Alexander, 2001; Mutti et al., 2003; Gamero et al., 2005; Pattison, 2005; Zavala et al., 2006c; Gamero et al., 2007, 2008; Zavala, 2008). Growing evidence emphasizes a close relationship between turbidity currents and rivers in flood in both modern (Nakajima, 2006) and ancient depositional settings (Mutti et al., 1996, 2003; Zavala et al., 2006b, c). Mutti et al. (2003) discussed the importance of flood-dominated fluvial-deltaic systems and their genetic relationship with hyperpycnal depositional models in shallow- and deep-water marine basins.

The occurrence of hyperpycnal flows in marine basins was initially received with skepticism (Nakajima, 2006), but it has been recognized at least since the published works by Mulder et al. and Mutti et al. in 2003 (Plink-Bjorklund and Steel, 2004; Gamero et al., 2005; Nakajima, 2006; Zavala et al., 2006c, 2007; Gamero et al., 2007). The origin of the long meandering submarine channels stemming from deltas, now widely attributed to sustained turbidity currents, was heavily debated a quarter of a century ago (Pickering and Hiscott, 1985).

Extensive work in outcrops and core studies (Mulder and Alexander, 2001; Gamero et al., 2005; Zavala et al., 2006a, b, c, 2007; Zavala, 2008) show that sedimentary facies related to quasi-steady hyperpycnal flows are very distinctive and could be easily differentiated from surge-like (resedimented) turbidite flows. A hyperpycnal flow is a land-derived relatively slow-moving

turbulent flow carrying interstitial fresh water basinward (Hesse et al., 2004; Mansurbeg et al., 2006). According to Zavala et al. (2006c), the movement of hyperpycnal flows does not require steep slopes because the energy of the flow is maintained by the river discharge during a flood, and the distance reached by these flows will be more dependent on the duration of the flood event.

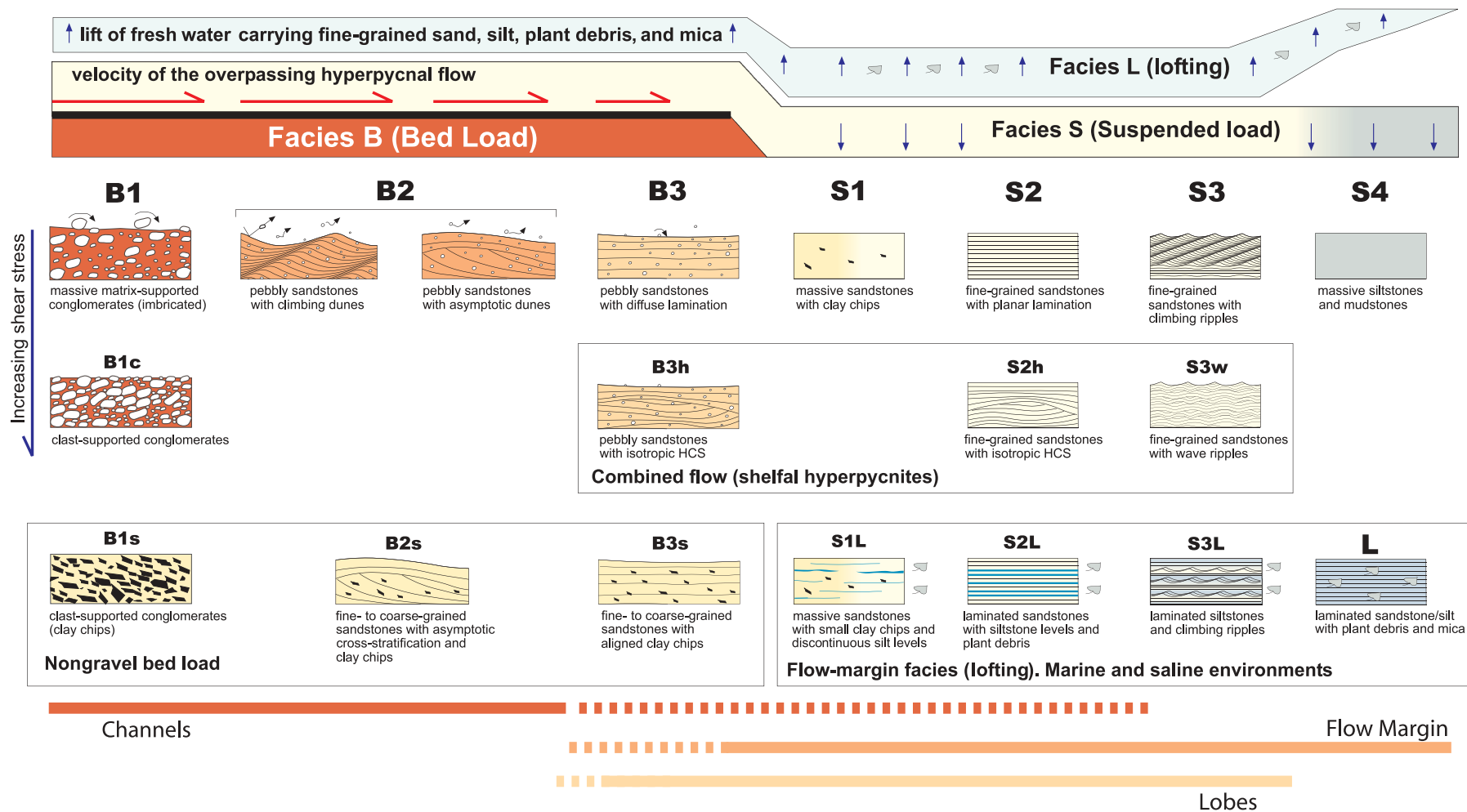
Zavala (2008) and Zavala et al. (2011) introduced a genetic facies tract for the analysis of sustained turbulent (noninertial) hyperpycnal flow deposits (Figure 5). This hyperpycnal facies tract is composed of three main genetically related facies groups termed B, S, and L, corresponding to bed-load, suspended-load, and lofting transport processes, respectively. This genetic facies model was followed in this study for the analysis of the Oilbird field.

## **DATA AND METHODOLOGY**

A sedimentologic interpretation was conducted in the Pliocene B4 reservoir sand at the Oilbird field (Figure 2). The general stratigraphy of the main reservoir sandstones in the Oilbird field are shown in the type log of Figure 3. Integration of multiple data including open-hole logs, core descriptions, borehole images, mud logs, and biostratigraphic interpretations was used to develop a new depositional model. Table 1 summarizes the data available including the interval of image data for each well. A total of 1149 m (3770 ft) of image data together with 18 m (60 ft) of core data were used to develop the sedimentologic model of the B4 sand. Borehole electrical imagery, integrated with selective conventional core data, constitutes a very powerful and effective technique for use in detailed reservoir characterization and further field development.

The methodology used in this study included the following:

- 1) Detailed facies analysis of 18 m (60 ft) of core data included the identification of facies and facies associations. The different facies were described and interpreted on the basis of the sedimentary processes involved during their origin. Facies associations were interpreted based on the genetically oriented facies tract (Zavala, 2008; Zavala et al., 2011) proposed for the analysis of hyperpycnal systems.
- 2) Recognition of core-based facies on the images was based on a detailed core-to-image- and -to-log calibration. As a result, an image-based facies



**FIGURE 5.** Genetic facies tract for the interpretation of hyperpycnal deposits (Zavala, 2008; Zavala et al., 2011). Type B facies relates to bed-load processes at the base of an overpassing long-lived turbulent flow. Type S facies originate from the sedimentation of sand-size suspended materials carried in the turbulent flow. Type L facies relates to fallout from lofting plumes. These facies are common in hyperpycnal flows entering a marine basin. HCS = hummocky cross-stratification.



**Table 1.** Summary of the available data for each well.

<i>Well Name</i>	<i>Open-Hole Logs</i>	<i>Mud Logs</i>	<i>Core Descriptions</i>	<i>Biostratigraphic Report</i>	<i>Borehole Images</i>	<i>Total Image (ft)</i>
Well 1	x			x		
Well 2	x	x			x	970
Well 3	x	x				
Well 4	x	x	x		x	853
Well 5	x	x			x	1740
Well 6	x	x				
Well 7	x	x			x	207

classification was used to interpret the remaining 1149 m (3770 ft) of image data.

- 3) Static and dynamic normalized borehole images were interpreted in conjunction with open-hole logs, such as gamma ray (GR), neutron-porosity, bulk density, and resistivity. Manual dip data were extracted directly from 1149 m (3770 ft) of borehole image data. The sedimentologic descriptions from borehole image data were integrated with mud-log results and complemented by biostratigraphic analysis from one well.
- 4) Borehole image data were used to determine sediment transport directions. It is important to highlight that borehole images provide paleocurrent determinations and sand orientations that support the sedimentologic interpretation obtained from the analysis of conventional nonoriented cores.
- 5) Stratigraphic cross sections were built to analyze the lateral variations of different facies associations. This requires recognition of facies associations from well logs and image data.
- 6) Depositional units were recognized based on the vertical stacking of facies associations and the GR log patterns.
- 7) Generation of facies maps. Facies maps were useful to analyze lateral facies changes through time for the different reservoir units throughout the field.

## RESULTS


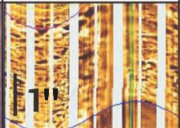







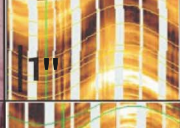





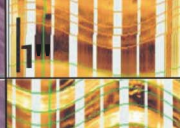

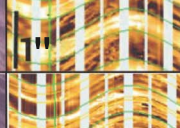

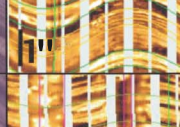

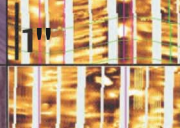
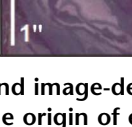

### *Core Data Analysis*

The B4 reservoir sand comprises a variety of facies dominated by fine- to very fine-grained sandstones. In this study, a total of 12 facies were recognized on the basis of their texture, sedimentary structures, and origin. These facies are (1) clay chip conglomerate

(B1s), (2) medium- to fine-grained sandstone with diffuse bedding (B3s), (3) medium- to fine-grained sandstone with asymptotic cross-stratification (B2s), (4) fine-grained massive sandstone (S1), (5) fine-grained sandstone with parallel laminations (S2), (6) fine-grained sandstone with climbing ripples (S3), (7) fine- to very fine-grained sandstone with hummocky cross-lamination (S2h), (8) fine- to very fine-grained sandstone with oscillatory ripples (S3w), (9) very fine-grained sandstones and siltstones with parallel laminations and abundant plant debris (S2L), (10) fine- to very fine-grained sandstones and siltstones with starved ripples (S3L), (11) thinly laminated siltstones with plant remains (L), and (12) very fine-grained sandstones and siltstones with water-escape structures and convolute bedding (Pd). Figure 6 summarizes the description and the origin of each recognized facies based on the main depositional processes involved during their accumulation. Main facies of the B4 reservoir were identified from an 18-m (60-ft)-long core acquired in well 4 (Figure 2). Core study was performed by core descriptions and continuous core photographs. Unfortunately, the core interval covers only 18 m (60 ft) of the lower part of the B4 reservoir sandstone. This core shows that the lower part of the B4 reservoir sandstone in well 4 is dominated by rhythmic, fine- to very fine-grained, parallel-laminated and massive sandstones interbedded with plant-derived carbonaceous material and thinly laminated sandstones and siltstones. As shown in Figure 6, the origin of these facies could be related to long-lived and land-derived hyperpycnal flows (Zavala et al., 2011).

### *Borehole Image Analysis*

Core interpretation was calibrated with the borehole image data acquired in well 4, which allowed the identification of 12 image-based facies (Figure 6).

Facies	Core Photo	Image	Lithology	Sedimentary Structures	Origin
B1s			Clay chip conglomerates within a medium-grained sandstone matrix.	Clasts alignment	Bed-load transport from an overpassing quasi-steady turbulent flow, over a consolidated substrate.
B3s			Medium- to fine-grained sandstones.	Crude plane parallel stratification	Bed-load transport from an overpassing quasi-steady turbulent flow, over a consolidated substrate.
B2s			Medium- to fine-grained sandstones.	Asymptotic cross-stratification	Bed-load transport from an overpassing quasi-steady turbulent flow, over a consolidated substrate.
S1			Fine-grained sandstones with floating clay chips.	Massive	Traction plus fallout from an overpassing quasi-steady turbulent flow.
S2			Fine-grained sandstones.	Parallel lamination	Traction plus fallout from an overpassing quasi-steady turbulent flow.
S3			Fine- to very fine-grained sandstones.	Climbing ripples	Traction plus fallout from an overpassing quasi-steady turbulent flow.
S2h			Fine- to very fine-grained sandstones.	Hummocky cross-stratification	Combined unidirectional flow and an oscillatory component flow.
S3w			Fine- to very fine-grained sandstones.	Oscillatory ripples	Traction plus fallout from an overpassing quasi-steady turbulent flow combined with an oscillatory component.
S2L			Fine- to very fine-grained sandstones interbedded with sandstones.	Parallel laminations interbedded with laminated siltstones and plant remains	Traction plus fallout from an overpassing quasi-steady turbulent flow plus precipitation from lofting plumes.
S3L			Fine- to very fine-grained sandstones interbedded with sandstones.	Ripple laminations interbedded with laminated siltstones and plant remains	Traction plus fallout from an overpassing quasi-steady turbulent flow plus precipitation from lofting plumes.
L			Light gray siltstones with plant remains.	Thinly laminated	Precipitation from lofting plumes.
Pd			Very fine-grained sandstones and laminated siltstones.	Water-escape structures and convolute bedding.	Water-escape structures is related to high sedimentation rates formed shortly after deposition.

**FIGURE 6.** Core- and image-derived facies scheme recognized from well data in the Oilbird field. It summarizes the description and the origin of each recognized facies based on the main depositional processes involved during their accumulation. HCS = hummocky cross-stratification.



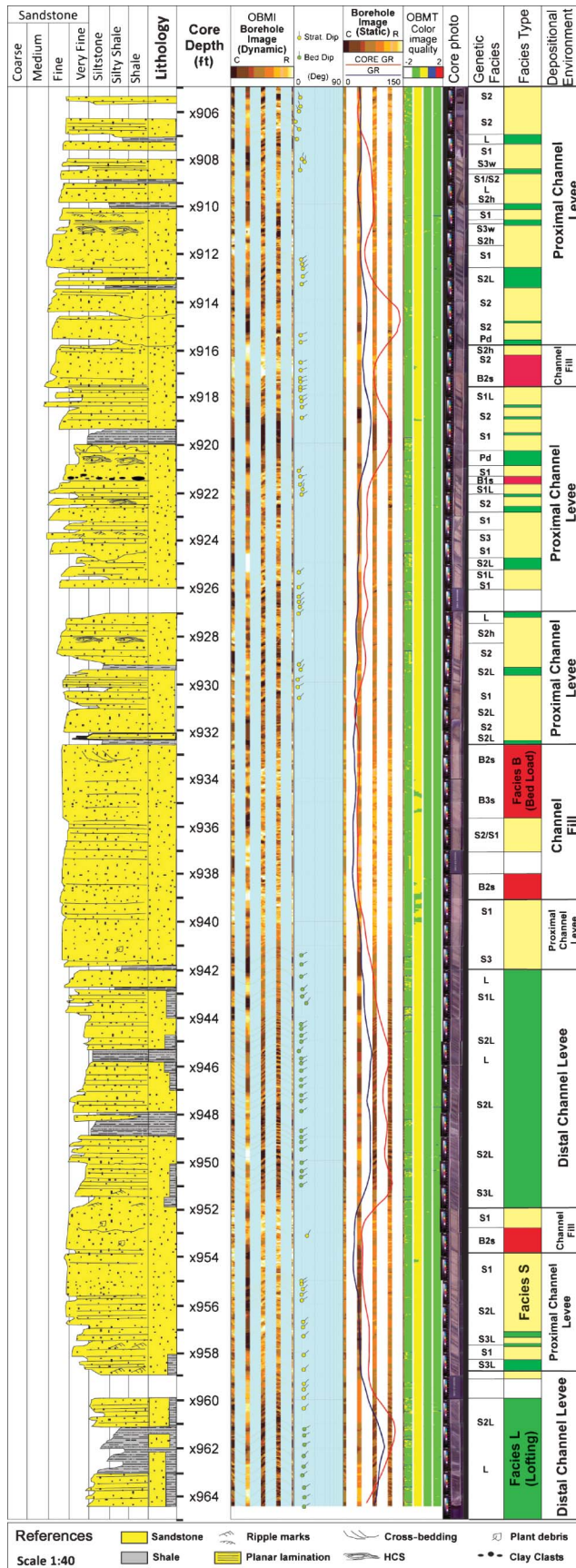
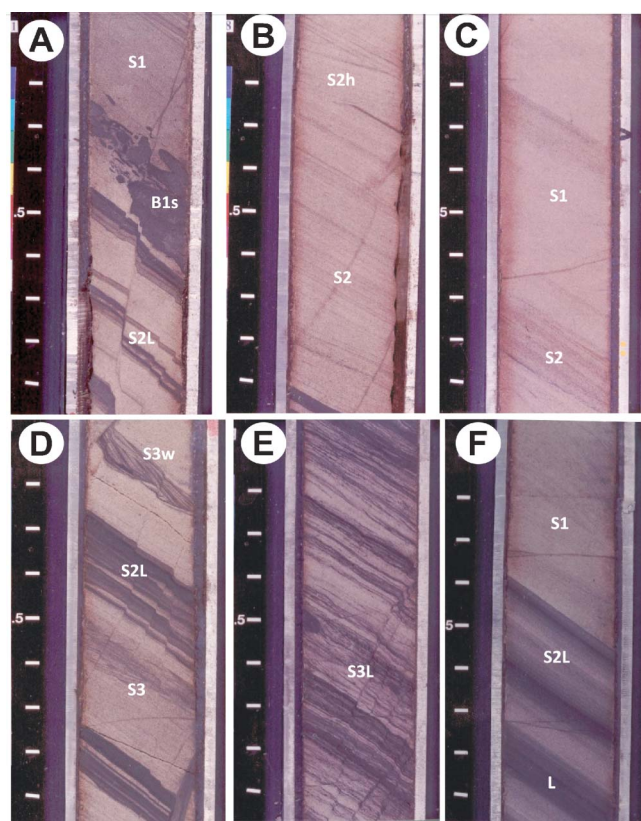


Figure 6 shows the image-based facies together with the core-based facies. These image-based facies were recognized on the basis of their texture, sedimentary structures, and origin. Sedimentary structures, such as cross-laminations, appear as sine-shaped bands of varying electrical contrast on dynamic normalized images. Dynamic normalization or image enhancement processing is used to bring out the details and is useful for detailed sedimentologic interactive analysis on the Image Examiner Workstation (Contreras and Gamero, 2000). The interpreter interactively fits a sine curve over each sedimentary structure to generate its orientation and assigns it to a specific sedimentologic category, such as planar lamination, cross-lamination, hummocky cross-stratification, and cross-bedding. The texture information in the wells with no core data was obtained from mud-log data analysis. Paleocurrent data were obtained by fitting a sine curve over the cross-bedding and cross-lamination structures providing orientation data. A structural dip removal was applied to determine the true paleocurrent orientation before being structurally altered.

This calibration permitted the identification of 12 image-based facies (Figure 6). Figure 7 shows the core-to-image calibration and the facies interpretation performed in well 4. The core-to-image calibration method is very important because it allows the extrapolation of the facies identified from the core throughout the 1149 m (3770 ft) of borehole image data without any additional core information. A new image-based facies scheme derived from image and core data was generated for the B4 sandstones in the Oilbird field based on the origin of the sedimentary structures. The interpreter's experience is important because of the possibility of recognizing a wide

**FIGURE 7.** Sedimentologic data sheet based on core and image calibration of well 4. The first track on the left shows a lithologic column generated from core photographs and core descriptions. The second track indicates the core depth, the third track the dynamic normalized borehole image, the fourth track the manual dip interpretation, and the fifth track the static normalized image. The sixth track shows the quality control of the image, in two colors: green indicates good quality; yellow indicates intermediate quality. The seventh track depicts the core photographs. The eighth, ninth, and tenth tracks represent the sedimentary facies, color-coded facies type, and depositional environment, respectively. Descriptions of the genetic facies are found in Figures 5 and 6. C = conductive; R = resistive; HCS = hummocky cross-stratification; GR = gamma ray; Strat. = stratigraphic; Deg = degree; OBMI = Oil-Base Microlmager (OBMI™) manufactured by Schlumberger.



**FIGURE 8.** Core photographs showing examples of the main sedimentary facies recognized in the analyzed core. (A) Clay clast conglomerate within a massive to laminated, fine-grained sandstone, interbedded with organic-rich silty laminations. (B) Parallel-laminated fine-grained sandstones with hummocky cross-stratification (HCS) toward the top. (C) Massive fine-grained sandstones commonly associated with parallel-laminated fine-grained sandstones. (D) Oscillatory ripples (toward the top of the photograph) interbedded with thinly laminated carbonaceous rich siltstones and very fine-grained sandstones. Bioturbation is very scarce. (E) Heterolithic facies consisting of thinly laminated carbonaceous rich siltstones and very fine-grained sandstones interbedded with parallel- and ripple-laminated very fine-grained sandstones. (F) Thinly laminated carbonaceous-rich siltstones and very fine-grained sandstones overlain by massive fine-grained sandstones. No bioturbation is observed.

range of features in outcrop and core, therefore providing an accurate interpretation of borehole images (Contreras and Gamero, 2000).

High-resolution borehole electrical imagery is regarded as a powerful tool to improve sedimentologic models that, calibrated with core, can be useful for identifying facies and providing paleocurrent data that can support the sedimentologic interpretation derived from conventional core analysis (Gamero et al., 2000).

### **Biostratigraphic Data**

A biostratigraphic analysis was performed in the B4 reservoir sandstone on the discovery well 1 (Figure 2B). This study reported inner-to-outer neritic (shelfal) conditions during deposition of the sandstones.

### **Depositional Model**

A new depositional model was proposed for the B4 sandstone in the Oilbird field on the basis of integrating core data, borehole images, and cuttings descriptions. Sedimentologic evidences suggest that the origin of the B4 sandstones could be related to fluvial-derived long-lived hyperpycnal flow deposited in a shelfal setting. During the late Pliocene, the paleo-Orinoco River discharges generated hyperpycnal flows that extended into the Columbus Basin. As previously mentioned, the different facies types recognized in the B4 sandstone were related to sustained turbulent hyperpycnal flows carrying interstitial fresh water inherited from the direct fluvial discharge. The main facies types interpreted from core and borehole images (Figure 6) have been classified primarily into bed-load (B)-, suspended-load (S)-, and lofting (L)-derived transport mechanisms within a genetic facies tract developed for hyperpycnal flows (Zavala et al., 2011). Bed-load facies (B1s, B3s, B2s; Figures 6, 8) range from clay chip conglomerates with a medium-grained sandstone matrix to medium- to fine-grained sandstones. Sedimentary structures exhibit clast alignment (B1s; Figure 8A) and crude plane-parallel stratification/banding (B3s) to asymptotic cross-stratification (B2s). Bed-load facies are thought to have originated from bed-load transport from an overpassing quasi-steady turbulent flow, over a consolidated substrate. The B2s facies is related to the migration of straight or sinuous bed forms at the base of a long-lived turbulent flow carrying high suspended load.

Suspended-load facies (S1, S2, and S3; Figure 6) range from fine-grained sandstones with floating clay chips to fine- to very fine-grained sandstones. These facies exhibit sedimentary structures that range from massive (S1; Figure 8C) parallel lamination (S2; Figure 8B) to climbing ripples (S3; Figure 8D) and would have been deposited as a result of traction plus fallout from an overpassing quasi-steady turbulent flow. Experimental studies (Arnott and Hand, 1989; Sumner et al., 2008) have shown that massive sandstones will originate from a turbulent flow with a relatively high fallout rate ( $>0.44$  mm/s), and parallel-laminated sandstones will originate from lower rates of



sediment fallout ( $<0.44$  mm/s) with equivalent flow velocities. Lamination in these massive sandstones is diffuse and appears as a recurrent feature within the massive intervals. The recurrence of massive and parallel-laminated sandstones without any break indicates fluctuating fallout rates from an overpassing sustained turbidite flow. Occasionally, we could see changes from parallel-laminated into climbing-ripple sandstones, which may suggest variations in flow conditions (Zavala et al., 2006c). These internally complex beds are called “composite beds” (Zavala et al., 2007) and typically display a vertical succession of different facies showing cyclical recurrence and transitional to sharp passages between them.

The S2h and S3w facies (Figure 6) are composed of fine- to very fine-grained sandstones. Main sedimentary structures are hummocky cross-stratification and oscillatory ripple laminations, respectively. The occurrence of hummocky cross-stratification (S2h; Figure 8B) and oscillatory ripples (S3w; Figure 8D) could be indicative of shallow-water conditions (shelfal hyperpycnites) in confined depocenters. The evidence of wave reworking at the top of major sandstone bodies is not always related to continuous wave-diffusion processes, but instead a consequence of the final reworking by the oscillating component of a density flow. In most cases, the oscillating component can be induced in the receiving basin by the disturbance provoked by the volume of the incoming flow in shallow-water bodies (Mutti et al., 1994).

Lofting-related facies (L, S2L, and S3L facies; Figure 6) are composed of fine- to very fine-grained sandstones interbedded with light gray siltstones with carbonaceous material. The associated occurrence of plant debris also favored the interpretation of a direct fluvial supply by rivers in flood (hyperpycnal systems). Main sedimentary structures are parallel and ripple laminations interbedded with thinly laminated siltstones with carbonaceous material. In general, these deposits show very little to no bioturbation. The S2L and S3L facies (Figure 8E, F) resulted from traction plus fallout from an overpassing quasi-steady turbulent flow combined with precipitation from lofting plumes. According to Zavala et al. (2006b), lofting facies constitute a diagnostic evidence of hyperpycnal sedimentation in a marine environment, resulting in vertical and lateral relationships between lofting and suspended-load facies, termed S2/L (laminated sandstones with abundant plant debris and micas) and S3/L (siltstone levels interbedded with sandstones having small climbing ripples). Lofting facies are related to the suspended fallout of fine-grained materials

from lofting plumes. These plumes are related to the inverted buoyancy associated with the lift-up forces caused by the less dense interstitial fresh water contained in the hyperpycnal flow (Sparks et al., 1993; Hesse et al., 2004; Zavala et al., 2006b; Zavala et al., 2011).

The Pd facies (Figure 6) is composed of very fine-grained sandstones and laminated siltstones with water-escape structures and convolute bedding caused by high sedimentation rates.

The main facies types recognized in the B4 sandstone show a dominance of suspended-load processes (S and L facies types). Facies related to the fallout of suspended materials from turbulent flows predominate in the medium to distal part of the depositional system.

### *Facies Analysis*

This study applied a genetic facies approach for performing facies analysis and the further development of a depositional model. Zavala et al. (2011) proposed a genetic facies approach that distinguishes facies on the basis of the main transport mechanisms involved during their deposition, resulting in a conceptual-based classification.

Facies associations were identified based on GR log trends integrated with the vertical stacking of facies interpreted from borehole images, core data, cuttings description, and biostratigraphic data within a conceptual-based channelized flow system derived from outcrop analysis. Figure 9 shows the lateral distribution of facies and facies associations within a channelized flow system (Zavala et al., 2006c). Six facies associations were identified from the image analysis of the B4 sandstone (Figure 10). These facies associations are discussed below.

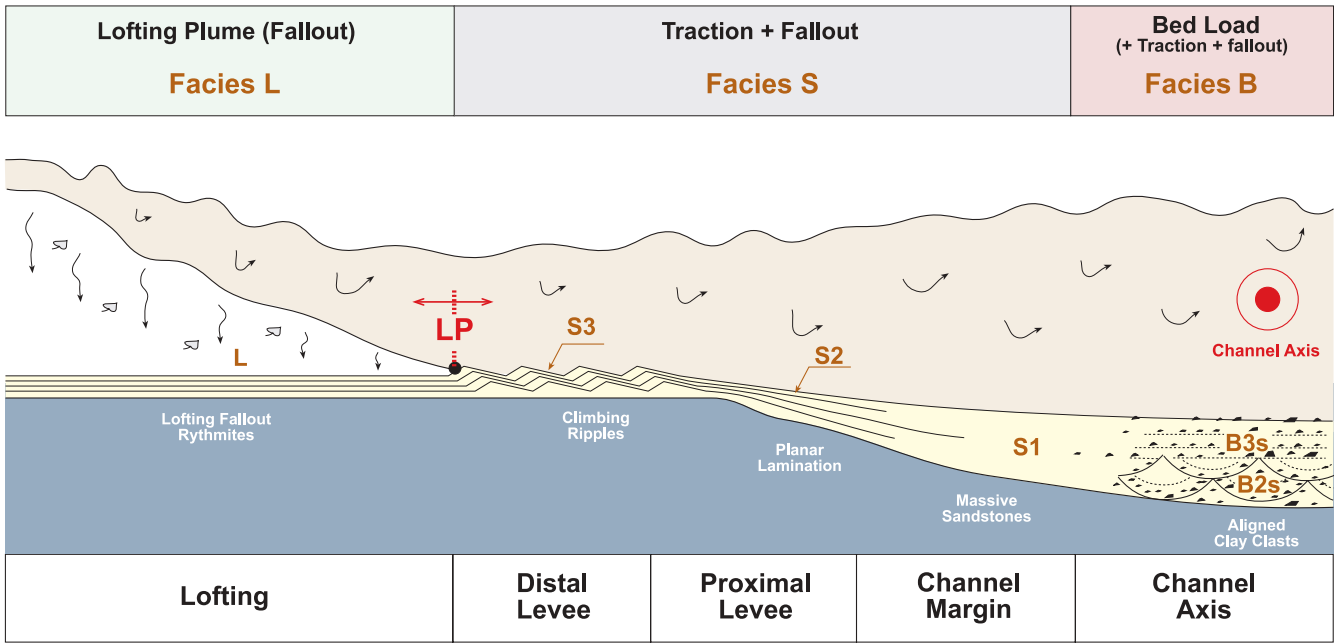
### *Shelfal Facies Association*

#### *Description*

Shelfal or background facies are composed of non-calcareous, dark gray, faintly to poorly laminated shales and siltstones (S4 facies).

This facies association appears in the images as poorly laminated to massive shales and siltstones having a relatively high GR response. These sediments might be moderately to highly bioturbated. Unfortunately, no highly bioturbated shelfal facies were identified in the core interval. Occasionally, images show interbedded deformed sandstone beds within the poorly layered siltstones and shales (Figure 10A).





**FIGURE 9.** Lateral distribution of facies associations in a channelized flow system (adapted from Zavala et al., 2011). The channel-axis association is characterized by alternating bed-load facies B1s, B2s, and B3s; the channel-margin association is characterized by facies S1 and possible association of B3s, S2, S2L, S3w, and S2h; proximal levee facies are characterized by alternating S-type facies (S1, S3, S2h, and S3w) and lofting facies (S2L); distal levee facies are characterized by lofting facies (S2L, S3L) alternating with suspended-load facies (S3, S2). Lofting facies represent the most lateral facies of a channelized flow and are characterized by facies L, S2L, and S3L. LP = lofting point.

**Interpretation**

This facies association originated by the settling of mud and silt from suspension clouds related to delta plumes during periods of low clastic input into the basin. These low clastic input periods coincided with maximum flooding surfaces, as suggested by biostratigraphic analysis.

**Lofting Facies Association**

**Description**

The lofting facies association is composed of thinly laminated light gray siltstones with plant remains and lignite. In the analyzed cores, this facies association commonly does not show any evidence of bioturbation, with remarkably well-preserved laminae. This facies association appears in the images as highly and thinly laminated siltstones, with corresponding high GR (Figure 10B).

**Interpretation**

Hesse et al. (2004) were the first to recognize lofting-related facies associated with ice-rafted debris in Pleistocene deposits of the Labrador Sea. The recognition

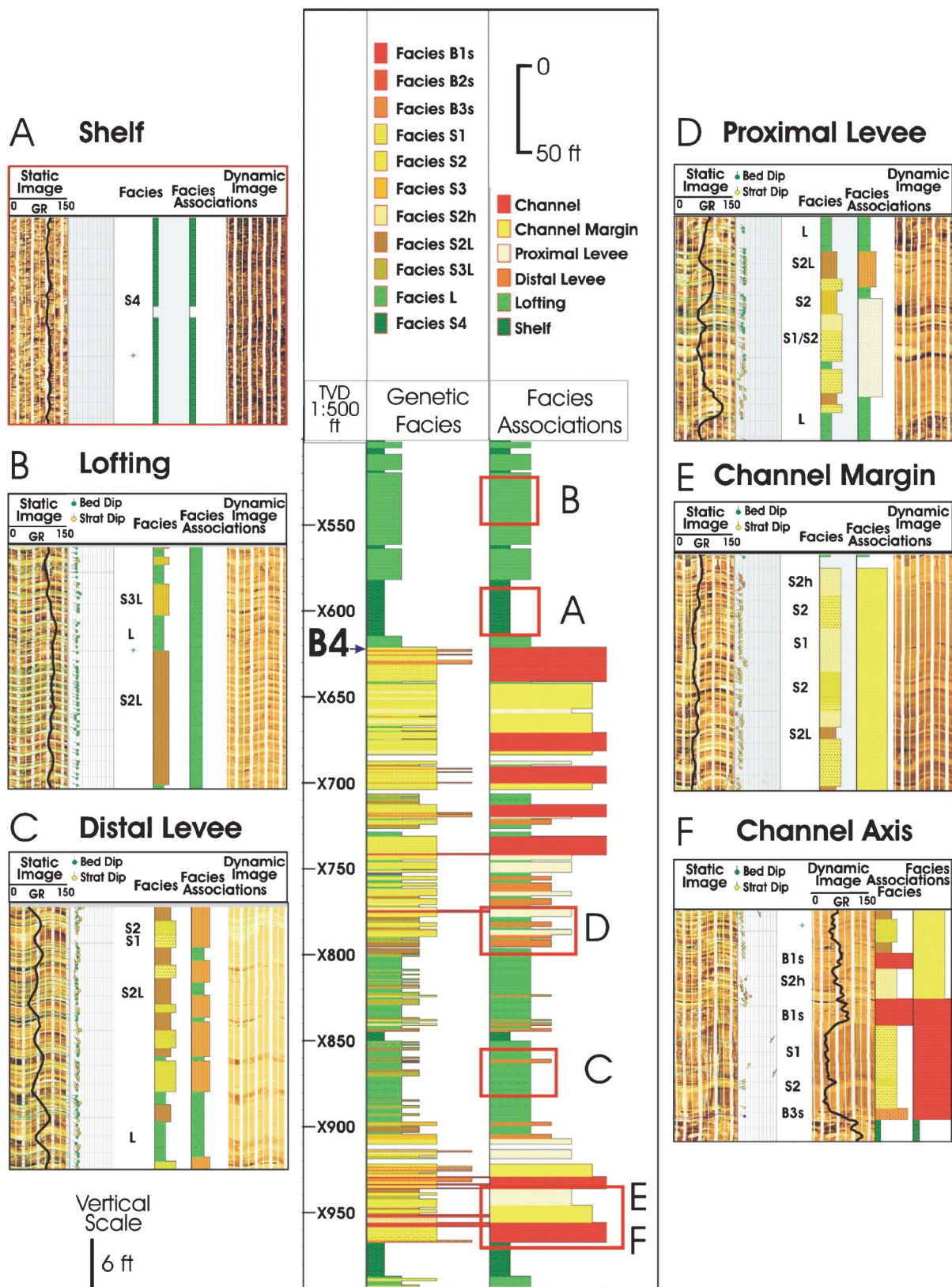
of lofting facies in marine environments is extremely important because it allows the diagnosis of a direct fluvial connection and a hyperpycnal origin for the associated deposits (Zavala et al., 2006b; Zavala, 2008). Lofting facies, in outcrops and cores, are composed of thinly laminated siltstones separated by thin intercalations of plant debris and micaceous, and their identification is very useful to predict the lateral occurrence of hyperpycnal channels in subsurface studies. This facies association is dominated by facies L commonly associated with facies S3L and S2L.

**Distal Levee Facies Association**

**Description**

The distal levee facies association is composed of stacked coarsening-upward successions (between 1 and 3 m [5 and 10 ft] thick), characterized from base to top by lofting facies (L, S3L), followed by 0.3- to 0.5-m (1- to 1.5-ft)-thick sharp-based, parallel-laminated, very fine-grained sandstones interbedded with thinly laminated argillaceous siltstones (S2L facies; Figure 10C). These facies appear in the images as highly and thinly laminated siltstones that grade

## FACIES ASSOCIATIONS - B4 SAND



**FIGURE 10.** Summary of main characteristics of the six facies associations described and interpreted for the B4 sandstone in the Oilbird field. It shows an example of the main characteristics of each facies association, in terms of gamma ray (GR) log trends, static and dynamic normalized image responses, and vertical stacking of facies interpreted from borehole images. TVD = true vertical depth; Strat = stratigraphic.

upward into 0.3- to 0.5-m (1- to 1.5-ft)-thick parallel-laminated sandstones, composed of a small-scale coarsening-upward (funnel-shaped) GR pattern.

### ***Interpretation***

This facies association is characterized by traction plus fallout processes that alternate with pure fallout from lofting plumes. The complex internal characteristics of these deposits could have originated from fluctuations in velocity and concentration during a single hyperpycnal discharge. This facies association is interpreted as having accumulated in a distal levee of a channelized system.

### ***Proximal Levee Facies Association***

#### ***Description***

The proximal levee facies association is composed of stacked coarsening- and thickening-upward successions (between 3 and 8 m [10 and 26 ft] thick), characterized from base to top by heterolithic or lofting facies (L, S2L, and S3L), consisting of sharp-based parallel or massive sandstones (up to 0.5 m [1.5 ft] thick) interbedded with thinly laminated shales and siltstones (up to 0.3 m [1 ft] thick), followed by 0.6- to 1-m (2- to 4-ft)-thick sharp-based ripple- to parallel-laminated sandstones (facies S2 and S3) (Figure 10D). This facies association appears in the images as a thinly horizontally layered interval that grades upward into 0.3- to 0.6-m (1- to 1.5-ft)-thick parallel and/or ripple-laminated sandstones interbedded with thinly horizontally layered beds, overlain by 0.6- to 1-m (2- to 4-ft)-thick parallel to massive sandstone beds. This facies association shows a coarsening-upward (funnel-shaped) GR pattern.

#### ***Interpretation***

This facies association is mostly composed of facies types originated by traction plus fallout processes with minor intercalations of lofting-related deposits. These characteristics suggest a marginal (lateral) position with respect to the main flow, and these deposits are interpreted as having accumulated in proximal levee areas (thickening-upward successions) located proximal to a channelized system.

### ***Channel-margin Facies Association***

#### ***Description***

This facies association is composed of stacked fining- and coarsening-upward successions (between 1 and 4 m [4 and 14 ft] thick), characterized by a vertical

recurrence of parallel-laminated and massive sandstones (S1 and S2 facies) interbedded with thin (<0.3-m [1-ft]-thick) shale/siltstones/carbonaceous levels (S1/L). The recurrence of these facies creates thick (>15-m [50-ft]-thick) internally complex sandstone beds with no clear facies boundaries, defined as composite beds by Zavala et al. (2007) (Figure 10E). These facies appear in the images as interbedded, parallel-laminated, and massive sandstones interbedded with thin horizontal beds. These deposits may show stacked coarsening-upward and fining-upward GR patterns.

#### ***Interpretation***

Composite beds typically display a vertical succession of different facies, showing cyclical recurrence and transitional to sharp passages between them. These cyclical and gradual changes are the result of near-continuous deposition from a fluctuating quasi-steady turbulent flow. This facies association is laterally related to amalgamated channel-fill facies. In this facies association, composite beds are almost entirely composed of suspended-load facies (S1, S2, and S3).

### ***Channel-axis Facies Association***

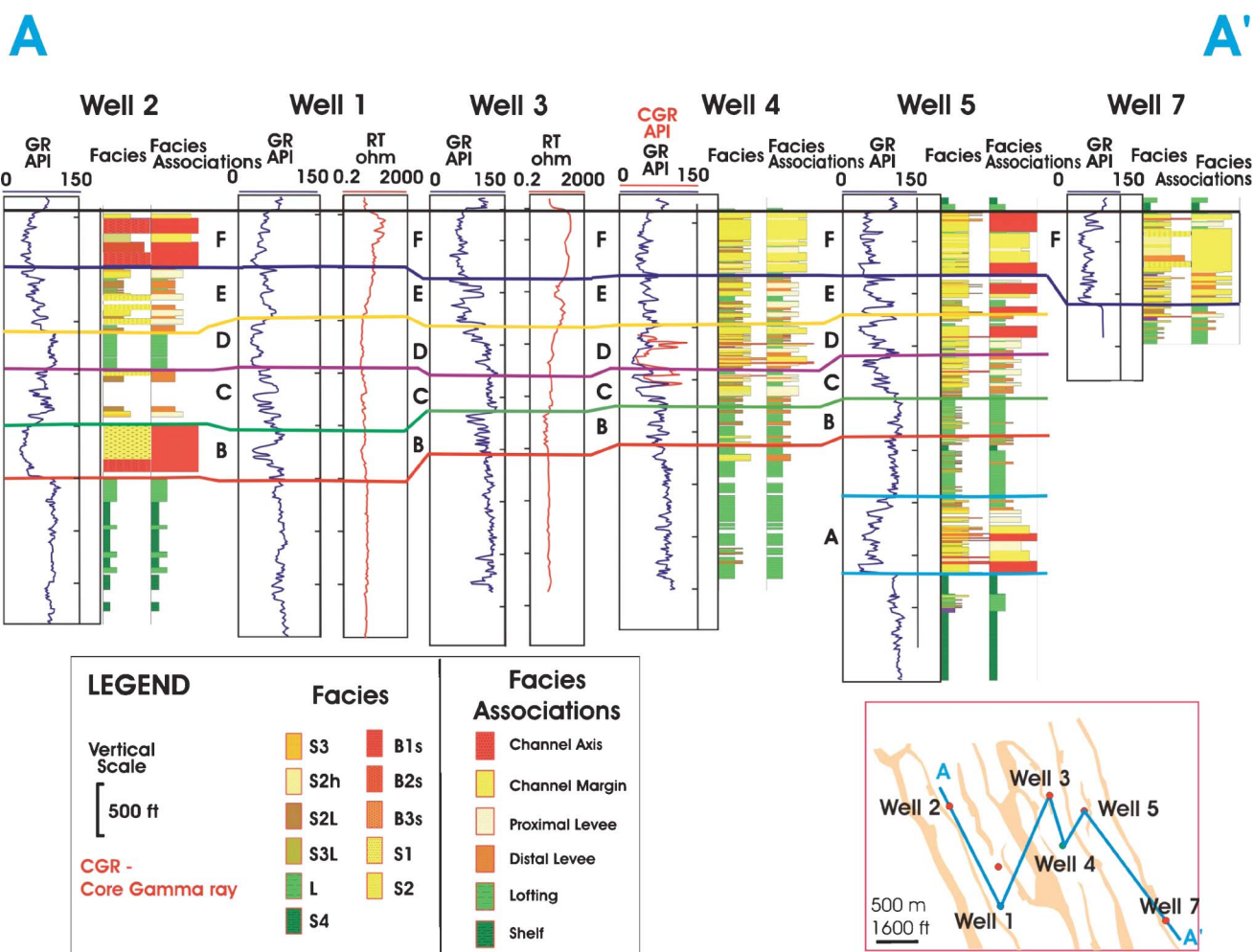
#### ***Description***

The channel-axis facies association is composed of stacked thinning-upward successions (between 6 and 15 m [20 and 50 ft] thick), characterized from the base to the top by massive and stratified medium-grained sandstones interbedded with pebbly conglomerates and asymptotic cross-bedded sandstones and overlain by parallel-laminated sandstones interbedded with massive sandstones. This facies association shows composite beds with a predominance of bed-load facies (Figure 10F). This facies may appear over an erosive basal boundary, followed by parallel-bedded sandstones with interbedded aligned resistive clasts, cross-bedded sandstones, and parallel-laminated and massive sandstones interbedded with thin horizontal beds. This facies association commonly shows a blocky to fining-upward GR pattern.

#### ***Interpretation***

This facies association is interpreted as channel-axis deposits. Channel axis is dominated by bed-load facies (B2s, B3s, and B1s). In this case, composite beds can be very thick (up to 15 m [50 ft] thick), depending on the duration of the hyperpycnal flow and the available accommodation space. These composite beds evolve laterally into lofting rhythmite





**FIGURE 11.** Regional detailed stratigraphic cross section showing lateral variation of sedimentary facies, facies associations, and depositional units of the B4 sandstone in the Oilbird field. The depositional units, named A, B, C, D, E, and F, were recognized based on the vertical stacking of facies associations and the gamma ray (GR) log patterns. GR = gamma ray in API units; RT = Resistivity in ohm m units; CGR = core gamma ray in API units. The API unit is a measure of radioactivity used for natural gamma-ray logs.

packages. Composite beds are coarser grained and better developed in the center of the channelized flow (Zavala et al., 2007).

### Facies Maps

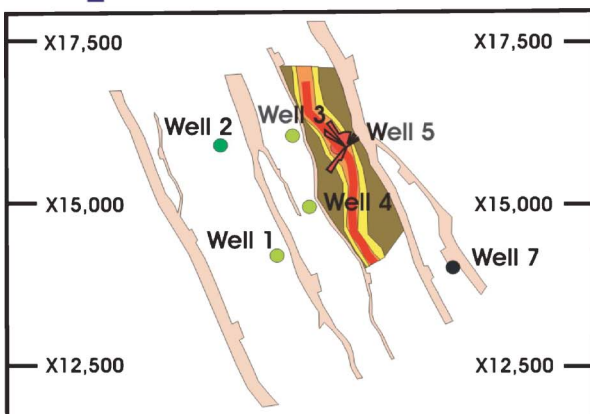
Based on the extrapolation of the image-derived facies associations and the GR log patterns, the B4 reservoir sand was further subdivided into six depositional units, denominated from base to top as A, B, C, D, E, and F. Figure 11 shows a cross section showing the main facies, facies associations, and depositional units interpreted on the B4 sandstone in the Oilbird field. Facies maps for the B4 reservoir have been developed and constrained by paleocurrent data derived from the analysis of image data.

Figure 12 shows the facies maps developed for each depositional unit.

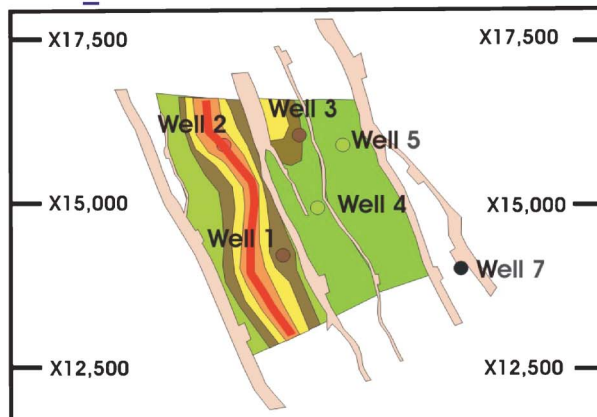
The depositional unit B4\_A is present only in well 5, which records the filling of a depositional low in this area as a north-northwest- to south-southeast-oriented channel (Figure 12A). Unit B4\_B is interpreted as being composed of channel-axis facies in well 2 and distal levee facies in wells 1 and 3. In wells 4 and 5, this unit is interpreted as lofting facies (Figure 12B). Unfortunately, no recorded paleocurrent data were available for this unit. Unit B4\_C is interpreted as distal levee facies in wells 1, 2, and 4. Lofting facies in well 3 and proximal levee facies were interpreted in well 5 (Figure 12C). Again, no paleocurrent data were available. Unit B4\_D is interpreted as channel margin in wells 1, 4, and 5, and proximal/

## Facies Map B4 Reservoir Sand

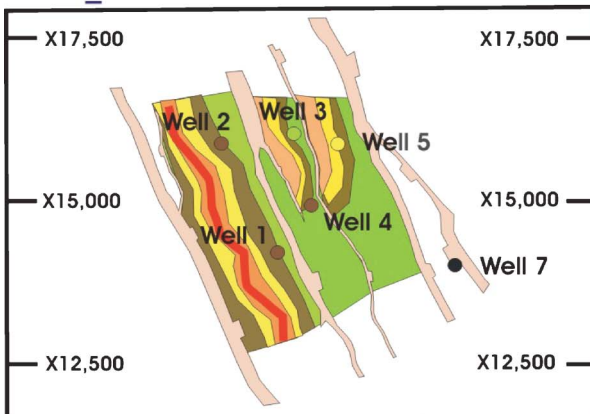
A. B4\_A



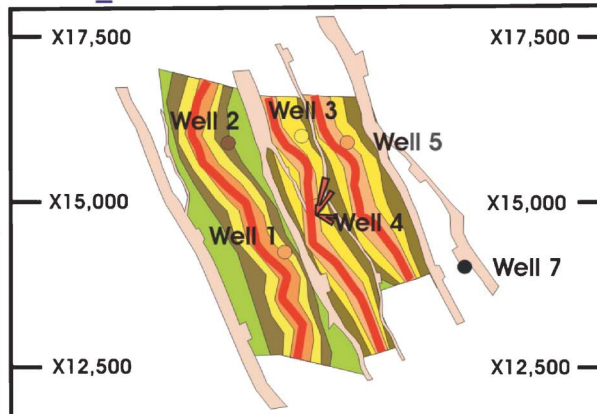
B. B4\_B



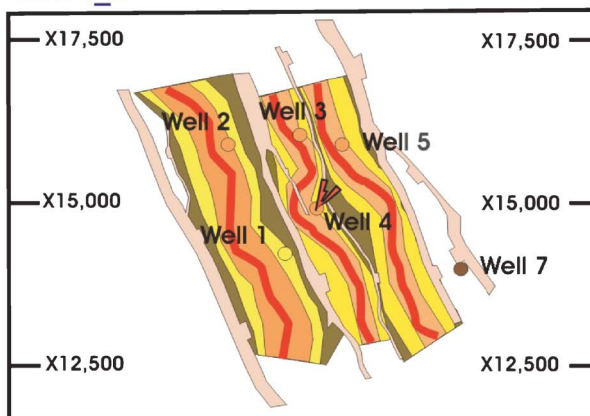
C. B4\_C



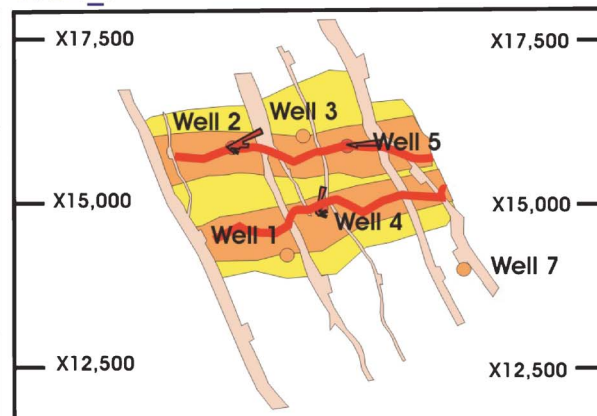
D. B4\_D



E. B4\_E



F. B4\_F



### Legend

### Facies Associations

- Shelf
- Proximal Levee
- Lofting
- Distal levee
- Channel Margin
- Channel Axis
- No logs

### Paleocurrent Data

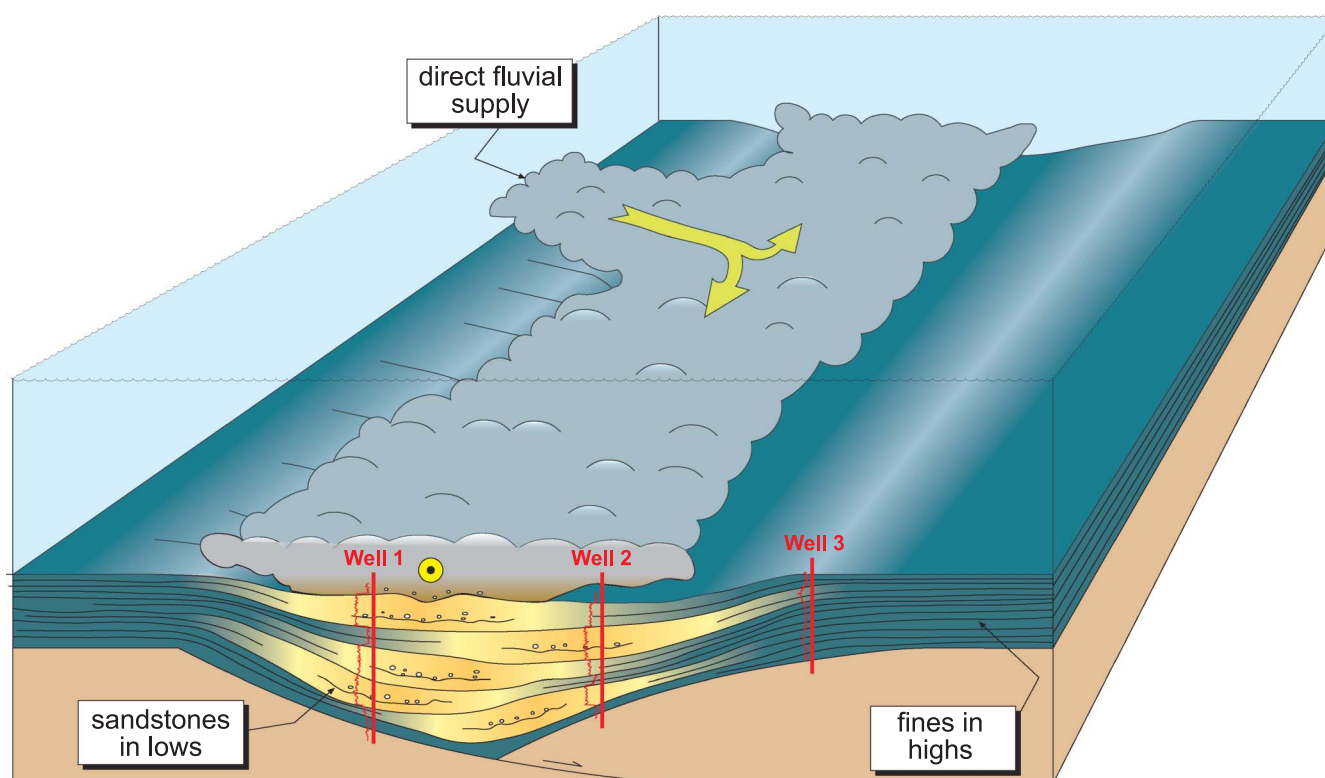


0 2500 ft  
Scale



**FIGURE 12.** Facies maps of the B4 sandstones in the Oilbird field. Each map shows a schematic depositional environment interpretation based on the sedimentologic study performed on each well. Paleocurrent data were overlain on the well location.





**FIGURE 13.** Schematic model of a fault-bounded depocenter filled by axial hyperpycnal flows.

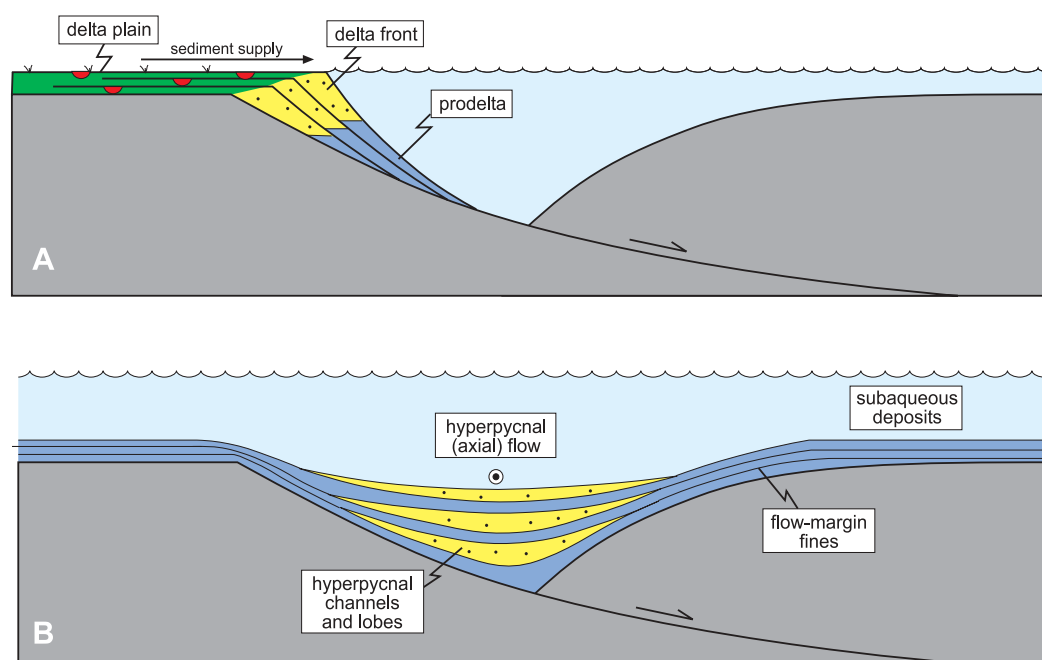
distal levee facies in wells 3 and 2, with paleocurrent data indicating a northeast-north-northeast and east-southeast orientation (Figure 12D). Unit B4\_E is interpreted as channel margin in wells 2, 3, 4, and 5, and proximal levee facies in wells 1 and 7. The interpreted channels show a northeast and east-northeast orientation based on paleocurrent data (Figure 12E). Finally, Unit B4\_F is interpreted as channel axis in wells 2, 4, and 5, and channel-margin facies in wells 1, 3, and 7; with paleocurrent data indicating east, northeast, and southeast paleocurrent directions (Figure 12F).

The B4 reservoir sandstone shows a progradational pattern, reflecting the filling of a fault-controlled depocenter or minibasin. The paleoflow data indicate axial transport parallel to the fault system, indicating that these faults were active, progressively creating accommodation space (Unit D; Figure 12). The upper sandstone represents the final stage of sand accumulation, evidenced by a change in transport direction toward the east (Unit F; Figure 12). A schematic model of the axial transport of these channelized flows filling the lows (Figure 13) shows that lofting facies can be interpreted either as related to a topographic high or to a lateral position with respect to the channelized flow. Although all the sedimentologic interpretations were consistent with the observations made on the

core and borehole images, a need to incorporate detailed mapping of these depositional units across the field using three-dimensional seismic data still exists. Unfortunately, seismic data in the Oilbird field are of poor quality and therefore not useful to support this model. However, based on seismic attribute analysis, a preferential north-south sand accumulation is seen (N. Lewis, 2007, personal communication), which may reflect the filling of these fault-bounded depocenters. In the literature, some examples that document axial transport of sediment gravity flows (Popescu et al., 2004; DeRuig and Hubbard, 2006) exist.

### *Implications in Reservoir Distribution*

The hyperpycnal model introduces substantial changes for the prediction of the geometry and position of the sandstone accumulations, and understanding these changes will require detailed mapping of the associated paleotopography during deposition. Figure 14 is a conceptual model showing differences between a shelf-margin delta model and an axial hyperpycnal model. The axial filling of these fault-bounded depocenters (or minibasins) will control the geometry of the associated sand bodies with consequent changes in determining potential new plays for exploration. In the case of the line-source delta model (Figure 14A),



**FIGURE 14.** Schematic comparison between the conventional deltaic model for the Columbus Basin versus the new proposed model for the Oilbird field. (A) Line-source littoral delta model. (B) Hyperpycnal model.

it predicts the existence of sandstone accumulations on one side (one source point) of the receiving basin, whereas the lower parts of the lower paleotopography will be characterized by the accumulation of fine-grained deposits. However, the hyperpycnal model (Figure 14B) predicts the occurrence of sand accumulation in the lowest part of the paleolandscape, whereas the higher parts of the basin (margins) will be characterized by fine-grained sediments. Thus, the hyperpycnal model will represent a change in the prospectivity guide for new exploration plays. Understanding the evolution of the structures in the Oilbird field and its relationship with the creation of accommodation space will help predict the accumulation of sandstones and its distribution for future prospects.

## SUMMARY AND CONCLUSIONS

Calibration of full-hole core data to borehole image log data has been critical to understand the depositional environment of the Oilbird field sandstones. Interpretation of these data has led to the identification of 12 distinct genetic facies. These genetic facies were deposited by hyperpycnal flows related to the subaqueous extension of the paleo-Orinoco fluvial system. Sedimentary facies related to hyperpycnal systems are very distinctive and could be easily differentiated from episodic surgelike classic turbidites. The presence of sandstone beds showing a recurrence of massive and parallel-laminated structures indicates sustained or near-continuous deposition from a quasi-

steady turbulent flow. All reservoir sandstones show a progradational pattern, reflecting the filling of a fault-controlled depocenter. Paleoflow data indicate axial transport parallel to the fault system, indicating that these faults were active during deposition of these sandstones. The upper sandstones, located at the top of the progradational sequences, represent the final accumulation stage evidenced by a change of paleoflow from northwest-southeast toward the east. The hyperpycnal model introduces substantial changes for the prediction of the shape and location of sand accumulations. The axial filling of these fault-bounded depocenters results in different sand body geometries with substantial changes for the prediction of new exploration plays.

## ACKNOWLEDGMENTS

This chapter presents the results of a sedimentologic study on the Oilbird field for EOG Resources Trinidad Limited. Mark Larsen and Maria Lourdes Diaz de Gamero provided reviews of the manuscript. We thank EOG Resources Trinidad Limited for giving its permission to publish the results of this study.

## REFERENCES CITED

- Arnott, R. W. C., and B. M. Hand, 1989, Bedforms, primary structures and grain fabric in the presence of suspended sediment rain: *Journal of Sedimentary Petrology*, v. 69, p. 1062–1069.

- Babb, S., and P. Mann, 1999, Structural and sedimentary development of a Neogene transpressional plate boundary between the Caribbean and South American plates in Trinidad and the Gulf of Paria, *in* P. Mann, ed., Caribbean basins, sedimentary basins of the world: Elsevier Science B.V., v. 4, p. 495–557.
- Bates, C., 1953, Rational theory of delta formation: AAPG Bulletin, v. 37, p. 2119–2162.
- Bowman, A., 2003, Sequence stratigraphy and reservoir characterization in the Columbus Basin, Trinidad, Ph.D. dissertation, University of London, London, England, 530 p.
- Bowman, A., and H. Johnson, 2006, Storm-dominated shelf-edge deltas in a high-accommodation setting: An outcrop example from the Columbus Basin, Trinidad, West Indies: AAPG/GSTT Hedberg Research Conference, Port of Spain, Trinidad West Indies, AAPG Search and Discovery Article 90057, 1 p., [http://www.searchanddiscovery.net/abstracts/html/2006/hedberg\\_intl/abstracts/bowman.htm](http://www.searchanddiscovery.net/abstracts/html/2006/hedberg_intl/abstracts/bowman.htm) (accessed July 2010).
- Contreras, C. C., and H. Gamero, 2000, High-resolution borehole images as powerful reservoir characterization tools: Transactions of the GSTT 2000 SPE Conference, Port of Spain, Trinidad 10–13 July, 2000, [http://www.gstt.org/publications/transactions\\_of\\_gstt\\_2000\\_spe.htm](http://www.gstt.org/publications/transactions_of_gstt_2000_spe.htm) (accessed July 2010).
- DeRuig, M., and S. Hubbard, 2006, Seismic facies and reservoir characteristics of a deep-marine channel belt in the Molasse Foreland Basin, Puchkirchen Formation, Austria: AAPG Bulletin, v. 90, no. 5, p. 735–752, doi:10.1306/10210505018.
- Diaz de Gamero, M. L., 1996, The changing course of the Orinoco River during the Neogene: A review: Palaeogeography, Palaeoclimatology, Palaeoecology, v. 123, p. 385–402, doi:10.1016/0031-0182(96)00115-0.
- Gamero, H., C. C. Contreras, P. Pestman, and A. Mizobe, 2000, Borehole electrical images as a reservoir characterization tool in the Merecure Formation, Guarico 13 field, eastern Venezuela: VII Simposio Bolivariano, Exploracion Petrolera en las Cuencas Subandinas, Memoria, p. 620–641.
- Gamero, H., C. Zavala, and C. Contreras, 2005, A reinterpretation of the Misoa facies types: Implications of a new depositional model, Maracaibo Basin, Venezuela (abs.): 2005 AAPG International Conference and Exhibition, Evolving Stratigraphic Techniques and Interpretation III, Paris, [http://www.searchanddiscovery.net/documents/abstracts/2005intl\\_paris/gamero.htm](http://www.searchanddiscovery.net/documents/abstracts/2005intl_paris/gamero.htm) (accessed July 2010).
- Gamero, H., J. Reader, C. Izatt, C. Zavala, and C. Contreras, 2007, Herrera sandstones in the Southern Basin Area, Trinidad: Evidence of hyperpycnites deposited away from ancient Oficina delta systems in eastern Venezuela (abs.): AAPG Annual Meeting, Abstracts volume, p. 51, <http://www.searchanddiscovery.net/abstracts/html/2007/annual/abstracts/lbGamero.htm> (accessed July 2010).
- Gamero, H., N. Lewis, R. Welsh, C. Zavala, and C. Contreras, 2008, Evidences of a shelfal hyperpycnal deposition in the Pliocene sandstones in the Oilbird field, SE Coast, Trinidad: Impact on reservoir distribution and field re-development, *in* J. J. Ponce and E. B. Olivero, conveners, Conference Proceedings, Research: Sediment transfer from shelf to deep water: Revisiting the delivery mechanisms, March 3–7, 2008, Ushuaia-Patagonia, Argentina, Conference Proceedings, 4 p., AAPG Search and Discovery Article 90079, [http://www.searchanddiscovery.net/abstracts/html/2008/hedberg\\_argentina/extended/gamero/gamero.htm](http://www.searchanddiscovery.net/abstracts/html/2008/hedberg_argentina/extended/gamero/gamero.htm) (accessed July 2010).
- Gibson, R., K. E. Meisling, and J. C. Sydow, in press, Columbus Basin, offshore Trinidad: A detached pull-apart basin in a transpressional foreland setting, *in* A. Bally and D. Roberts, eds., Phanerozoic regional geology of the world: Columbus Basin, v. 3, Elsevier.
- Hesse, R., H. Rashid, and S. Khodabakhsh, 2004, Fine-grained sediment lofting from meltwater-generated turbidity currents during Heinrich events: Geology, v. 32, p. 449–452, doi:10.1130/G20136.1.
- Jackson, C., A. A. Zakaria, H. D. Johnson, F. Tongkul, and P. D. Crevello, 2009, Sedimentology, stratigraphic occurrence and origin of linked debrites in the west Crocker Formation (Oligo–Miocene), Sabah, NW Borneo: Marine and Petroleum Geology, v. 26, p. 1957–1973, doi:10.1016/j.marpetgeo.2009.02.019.
- Kneller, B., and M. Branney, 1995, Sustained high-density turbidity currents and the deposition of thick massive sands: Sedimentology, v. 42, p. 607–616, doi:10.1111/j.1365-3091.1995.tb00395.x.
- Lamb, M. P., and D. Mohrig, 2009, Do hyperpycnal-flow deposits record river-flood dynamics?: Geology, v. 37, p. 1067–1070, doi:10.1130/G30286A.1.
- Lamb, M. P., P. M. Myrow, C. Lukens, K. Houck, and J. Strauss, 2008, Deposits from wave-influenced turbidity currents: Pennsylvanian Minturn Formation, Colorado: Journal of Sedimentary Research, v. 78, p. 480–498, doi:10.2110/jsr.2008.052.
- Leonard, R., 1983, Geology and hydrocarbon accumulations, Columbus Basin, offshore Trinidad: AAPG Bulletin, v. 67, no. 7, p. 1081–1093.
- Mansurbeg, H., M. A. K. El-ghali, S. Morad, and P. Plink-Björklund, 2006, The impact of meteoric water on the diagenetic alterations in deep-water, marine siliclastic turbidites: Journal of Geochemical Exploration, v. 89, p. 254–258, doi:10.1016/j.gexplo.2006.02.001.
- Mulder, T., and J. Alexander, 2001, The physical character of subaqueous sedimentary density flows and their deposits: Sedimentology, v. 48, p. 269–299, doi:10.1046/j.1365-3091.2001.00360.x.
- Mulder, T., J. P. M. Syvitski, S. Migeon, J. C. Faugères, and B. Savoye, 2003, Marine hyperpycnal flows: Initiation, behavior and related deposits: A review: Marine and Petroleum Geology, v. 20, p. 861–882, doi:10.1016/j.marpetgeo.2003.01.003.
- Mutti, E., G. Davoli, and R. Tinterri, 1994, Flood-related gravity-flow deposits in fluvial and fluvio-deltaic depositional systems and their sequence-stratigraphic implications, *in* H. W. Posamentier and E. Mutti, eds.,

- Second High-Resolution Sequence Stratigraphy Conference, Tremp, Abstract Book: Italy, Instituto di Geologia, Universita di Parma, p. 137–143.
- Mutti, E., G. Davoli, R. Tinterri, and C. Zavala, 1996, The importance of ancient fluvio-deltaic systems dominated by catastrophic flooding in tectonically active basins: *Memorie di Scienze Geologiche*, Universita di Padova, v. 48, p. 233–291.
- Mutti, E., R. Tinterri, G. Benevelli, D. Di Biase, and G. Cavanna, 2003, Deltaic, mixed and turbidite sedimentation of ancient foreland basins: *Marine and Petroleum Geology*, v. 20, p. 733–755, doi:10.1016/j.marpetgeo.2003.09.001.
- Nakajima, T., 2006, Hyperpycnites deposited 700 km away from river mouths in the Central Japan Sea: *Journal of Sedimentary Research*, v. 76, p. 59–72.
- Pattison, S., 2005, Storm-influenced prodelta turbidite complex in the Lower Kenilworth member at Hatch Mesa, Book Cliffs, Utah: Implications for shallow marine facies models: *Journal of Sedimentary Research*, v. 75, no. 4, p. 420–439, doi:10.2110/jsr.2005.033.
- Pickering, K. T., and R. N. Hiscott, 1985, Contained (reflected) turbidity currents from the Middle Ordovician Cloridorme Formation, Quebec, Canada: An alternative to the antidune hypothesis: *Sedimentology*, v. 32, p. 373–394, doi:10.1111/j.1365-3091.1985.tb00518.x.
- Pindell, J. L., R. Higgs, and J. Dewet, 1998, Cenozoic palinspastic reconstruction, paleogeographic evolution and hydrocarbon setting of the northern margin of South America, in *Paleogeographic evolution and nonglacial eustasy, Northern South America*: SEPM Special Publication 58, p. 45–85.
- Plink-Björklund, P., and R. J. Steel, 2004, Initiation of turbidite currents: Outcrop evidence for Eocene hyperpycnal flow turbidites: *Sedimentary Geology*, v. 165, p. 29–52, doi:10.1016/j.sedgeo.2003.10.013.
- Popescu, I., G. Lericolais, N. Panin, and A. Normand, 2004, The Danube submarine canyon (Black Sea): Morphology and sedimentary processes: *Marine Geology*, v. 206, no. 1–4, p. 249–265, doi:10.1016/j.margeo.2004.03.003.
- Robertson, P., and K. Burke, 1989, Evolution of the southern Caribbean plate boundary, vicinity of Trinidad and Tobago: *AAPG Bulletin*, v. 73, no. 4, p. 490–509.
- Schumm, S. A., 1981, The evolution and response of the fluvial system, sedimentologic implications, in F. G. Ethridge and R. M. Flores, eds., *Recent and ancient non-marine depositional environments: Models for exploration*: SEPM Special Publication 31, p. 19–29.
- Sparks, R. S. J., R. T. Bonnecaze, H. E. Huppert, J. R. Lister, M. A. Hallworth, J. Phillips, and H. Mader, 1993, Sediment-laden gravity currents with reversing buoyancy: *Earth and Planetary Science Letters*, v. 114, p. 243–257, doi:10.1016/0012-821X(93)90028-8.
- Sumner, E. J., L. A. Amy, and P. J. Talling, 2008, Deposit structure and processes of sand deposition from decelerating sediment suspensions: *Journal of Sedimentary Research*, v. 78, p. 529–547, doi:10.2110/jsr.2008.062.
- Walker, R., 1996, Facies modeling and sequence stratigraphy: *Journal of Sedimentary Petroleum*, v. 60, p. 777–786.
- Wood, L., 2000, Chronostratigraphy and tectonostratigraphy of the Columbus Basin, Eastern offshore Trinidad: *AAPG Bulletin*, v. 84, no. 12, p. 1905–1928.
- Wood, L., and C. Roberts, 2001, Opportunities in a world-class hydrocarbon basin: Trinidad and Tobago's eastern offshore marine province: *Houston Geological Society Bulletin*, v. 43, no. 10, p. 37–45.
- Zavala, C., 2008, Toward a genetic facies tract for the analysis of hyperpycnal deposits, in J. J. Ponce and E. B. Olivero, conveners, *Conference Proceedings, Research Sediment transfer from shelf to deep water: Revisiting the delivery mechanisms: Ushuaia-Patagonia, Argentina*, Conference Proceedings, AAPG Search and Discovery Article 50075, 2 p., [http://www.searchanddiscovery.net/abstracts/html/2008/hedberg\\_argentina/extended/zavala/zavala.htm](http://www.searchanddiscovery.net/abstracts/html/2008/hedberg_argentina/extended/zavala/zavala.htm) (accessed July 2010).
- Zavala, C., M. Arcuri, and H. Gamero, 2006a, Toward a genetic model for the analysis of hyperpycnal systems (abs.): *Geological Society of America Abstracts with Programs*, v. 38, no. 7, p. 541, [http://gsa.confex.com/gsa/2006AM/finalprogram/abstracts\\_110453.htm](http://gsa.confex.com/gsa/2006AM/finalprogram/abstracts_110453.htm) (accessed July 2010).
- Zavala, C., H. Gamero, and M. Arcuri, 2006b, Lofting rhythmites: A diagnostic feature for the recognition of hyperpycnal deposits (abs.): *Geological Society of America Abstracts with Programs*, v. 38, no. 7, p. 541, [http://gsa.confex.com/gsa/2006AM/finalprogram/abstracts\\_110667.htm](http://gsa.confex.com/gsa/2006AM/finalprogram/abstracts_110667.htm) (accessed July 2010).
- Zavala, C., J. Ponce, D. Dritanti, M. Arcuri, H. Freije, and M. Asensio, 2006c, Ancient lacustrine hyperpycnites: A depositional model from a case study in the Rayoso Formation (Cretaceous) of west-central Argentina: *Journal of Sedimentary Research*, v. 76, p. 41–59, doi:10.2110/jsr.2006.12.
- Zavala, C., M. Arcuri, H. Gamero Díaz, and C. Contreras, 2007, The composite bed: A new distinctive feature of hyperpycnal deposition (abs.): *AAPG Annual Convention & Exhibition*, v. 16, p. 157, <http://www.searchanddiscovery.net/abstracts/html/2007/annual/abstracts/lbZavala.htm> (accessed July 2010).
- Zavala, C., M. Arcuri, M. Di Meglio, H. Gamero Diaz, and C. Contreras, 2011, A genetic facies tract for the analysis of sustained hyperpycnal flow deposits, in R. M. Slatt and C. Zavala, eds., *Sediment transfer from shelf to deep water—Revisiting the delivery system*: AAPG Studies in Geology 61, p. 31–51.